Stellar Dynamics and Structure of Galaxies

Star Clusters

Vasily Belokurov
vasily@ast.cam.ac.uk

Institute of Astronomy

Lent Term 2016

Outline I

Outline II

Globular Clusters

Globular clusters are approximately spherical, compact agglomerations of stars swarming around galaxies. They are as old as the galaxies themselves and provide unique clues to how the star formation and the galaxy formation proceeded in the ancient Universe.

Being old, spherical and devoid of Dark Matter, globular clusters are perfect environments to learn about the gravity works.

M15, Hubble

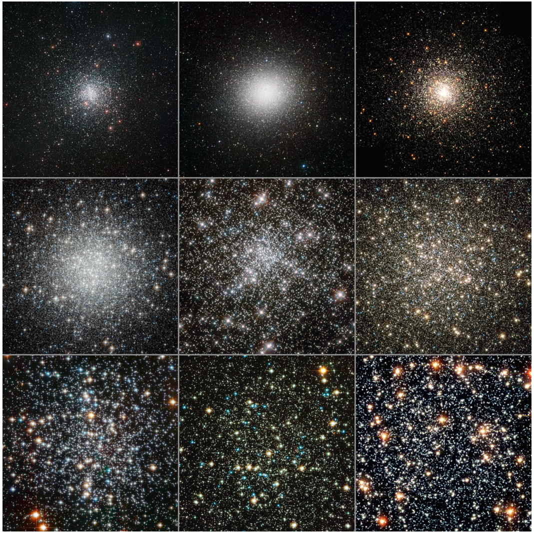

Top row: Messier 4 (ESO), Omega Centauri (ESO), Messier 80 (Hubble)
Middle row: Messier 53 (Hubble), NGC 6752 (Hubble), Messier 13 (Hubble)
Bottom row: Messier 4 (Hubble), NGC 288 (Hubble), 47 Tucanae (Hubble)

The Great Debate

26 April 1920, in the Baird auditorium of the Smithsonian Museum of Natural History.

"The Scale of the Universe"

Harlow Shapley

The nebulae are part of the large Milky Way system

Heber Curtis

The nebulae are "Island Universes" located at large distances away from the Galaxy

The Great Debate

- Vesto Melvin Slipher measured wavelength shifts of spiral nebulae
- Johannes C. Kapteyn advertised a small Milky Way centered on the Sun
- Adriaan van Maanen measured apparent rotation of spiral galaxies
- Knut Lundmark speculated that the dwarf novae might be so bright as to be detectable millions of light years from us

The Great Debate

- Shapley believes the Galaxy is tens of kpc across. "If spiral galaxies are like islands, then the Galaxy is a continent"
- Curtis's Milky Way is much smaller, only 10 kpc across

The Great Debate

- Resolved F, G and K stars in globular clusters. Shapley: these are giants, Curtis: these are dwarfs.
- Cepheids as distance indicators. Shapley: there is P-L relation. Curtis: parallaxes are too small, "more data needed".
- Spectroscopic parallaxes. Shapley: these are to be trusted. Curtis: to be trusted only within 100 pc.
- Interpretation of the star counts. Curtis: star counts suggest small MW, but would place the dust outside the stellar disk. Shapley: did not address the issue.
- Distribution of spiral nebulae on the sky. Shapley: "single system" - all is possible. Curtis: "neither impossible nor implausible" for the MW to have a dust ring around it.
- Nova brightness at maximum. Shapley: the implied real brightnesses would be totally ridiculous. Curtis: trust the calibration based on a handful of MW events.
- Large positive velocities of spiral nebulae. Shapley: repulsion by radiation pressure form the MW. Curtis: "I haven't a clue"
- Central location of the Sun. Shapley: an illusion caused the local star cloud. Curtis: this is God's own truth
- Rotational proper motions of spirals as measured by van Maanen. Shapley: a strong argument against opponent. Curtis: too dodgy

The Great Debate

The outcome?

- Both were mainly right, but also impressively wrong in some very important points.
- Right when relying on their own data, and wobbly when attempting to speculate based on the current theory.

The Great Debate

The State of the Art

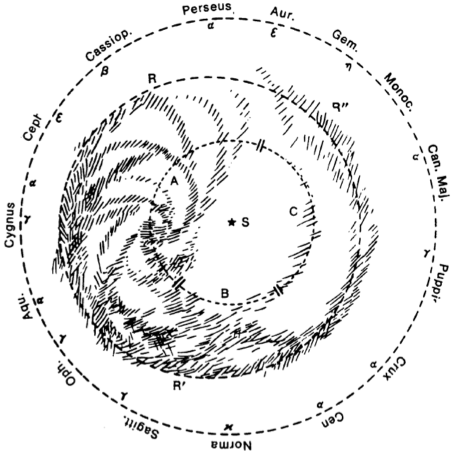

FIG. 2—Cornelius Easton's model of the Galaxy in 1900. He was the first to give the Milky Way spiral arms.

The Great Debate

The State of the Art

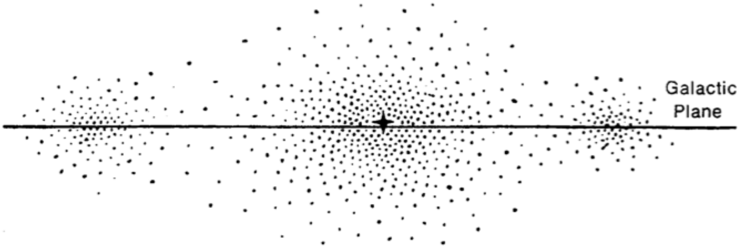

FIG. 3—Arthur Eddington's (1912) galaxy placed the Sun's position 60 LY above the center of the galactic plane.

The Great Debate

The State of the Art

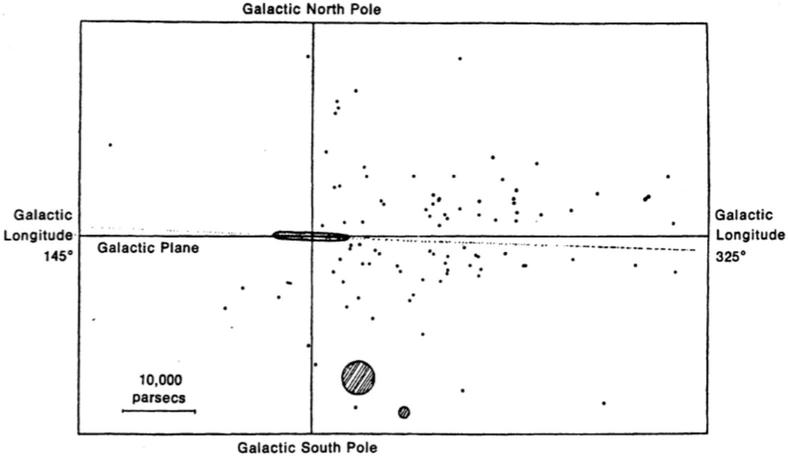

Trumpler's Galaxy with the Sun in the middle of Kapteyn Universe

The Great Debate

Shapley: The Sun lies in a nondescript location in the Galaxy.

This is a key part to a bigger Copernican Principle, that we live neither in the centre of the Solar System, our Galaxy, nor the Universe as a whole.

The Role of Star Clusters

- Galaxy structure
- Galaxy formation
- Stellar evolution
- Star formation

Galactic Structure

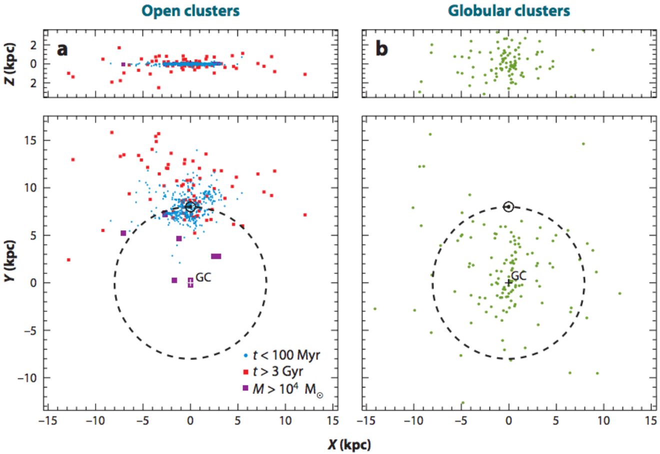

Portegies Zwart et al, 2010

Galactic Structure

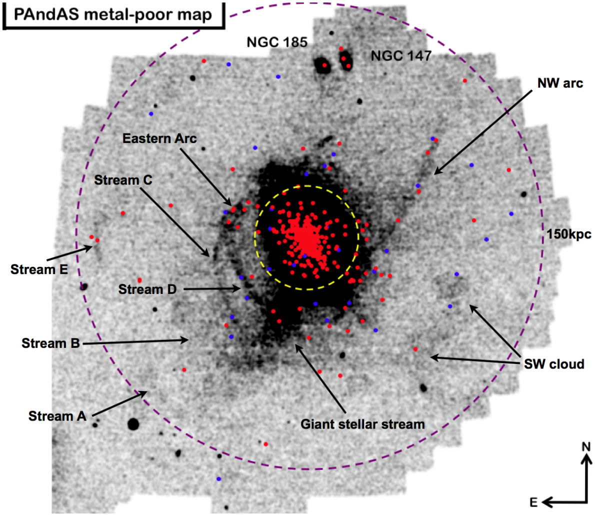

M. Irwin and PAndAS collaboration

Number of Globular Clusters per galaxy

- Milky Way: $100 < N < 200$
- Andromeda: $200 < N < 500$
- M 87: $N > 1000$

Number of Globular Clusters per galaxy

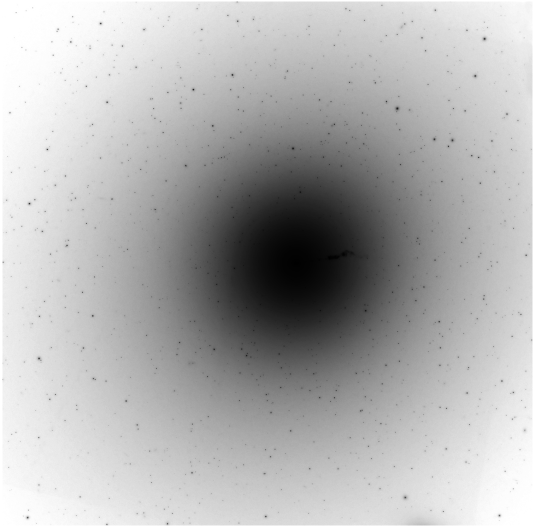

M87 globular clusters

Curious GC in M87

Astrophysics > Galaxy Astrophysics

A Globular Cluster Toward M87 with a Radial Velocity < −1000 km/s: The First Hypervelocity Cluster

Nelson Caldwell (CfA), Jay Strader (Michigan St), Aaron J. Romanowsky (San Jose St/Santa Cruz), Jean P. Brodie (Santa Cruz), Ben Moore (Zurich), Jurg Diemand (Zurich), Davide Martizzi (Berkeley)

(Submitted on 25 Feb 2014)

We report the discovery of an object near M87 in the Virgo Cluster with an extraordinary blueshift of −1025 km/s, offset from the systemic velocity by >2300 km/s. Evaluation of photometric and spectroscopic data provides strong evidence that this object is a distant massive globular cluster, which we call HVGC-1 in analogy to Galactic hypervelocity stars. We consider but disfavor more exotic interpretations, such as a system of stars bound to a recoiling black hole. The odds of observing an outlier as extreme as HVGC-1 in a virialized distribution of intracluster objects are small; it appears more likely that the cluster was (or is being) ejected from Virgo following a three-body interaction. The nature of the interaction is unclear, and could involve either a subhalo or a binary supermassive black hole at the center of M87.

Comments: submitted to ApJL, comments welcome
Subjects: **Galaxy Astrophysics (astro-ph.GA)**; Cosmology and Extragalactic Astrophysics (astro-ph.CO)
Cite as: arXiv:1402.6319 [astro-ph.GA]
(or arXiv:1402.6319v1 [astro-ph.GA] for this version)

Caldwell et al

Curious GC in M87

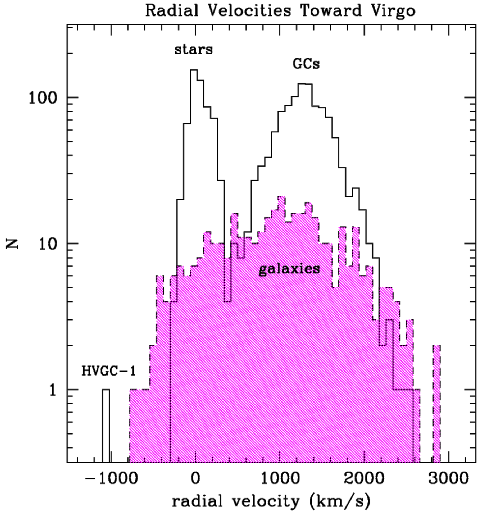

Caldwell et al

Color-Magnitude Diagram

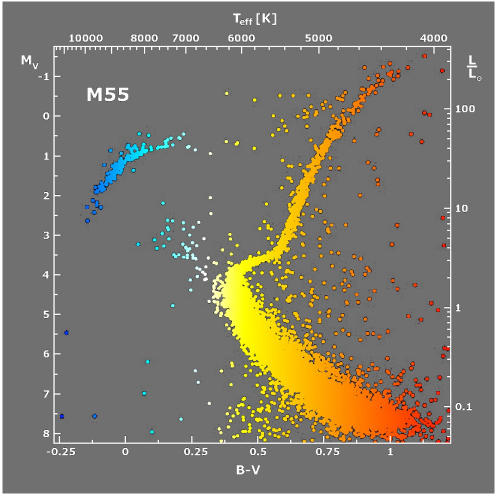

Stellar Luminosity Function

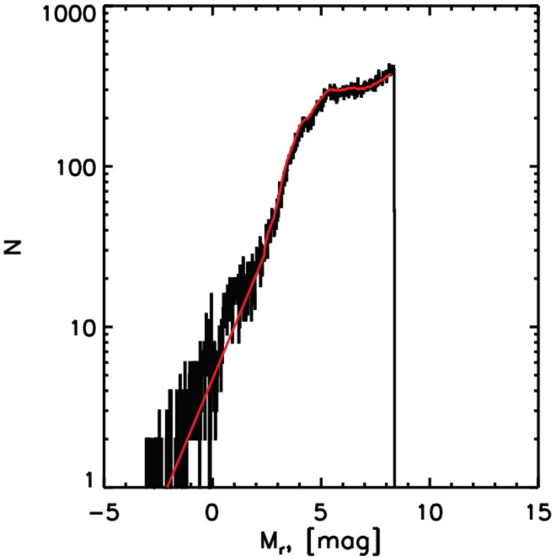

Color-Magnitude Diagram

M92 globular cluster

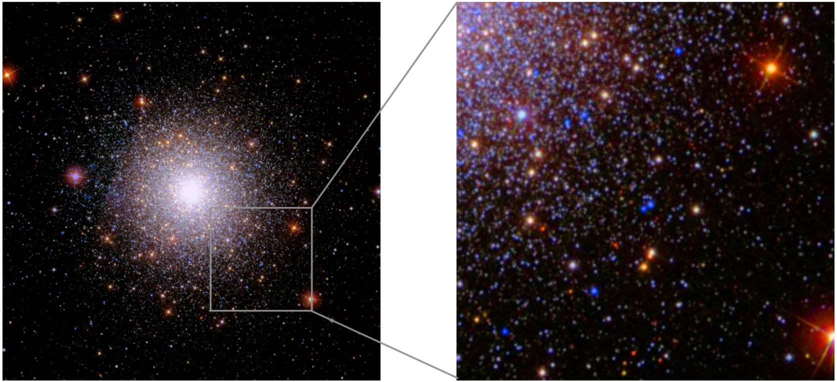

Cluster Ages

Open VS globular ages. Easy!

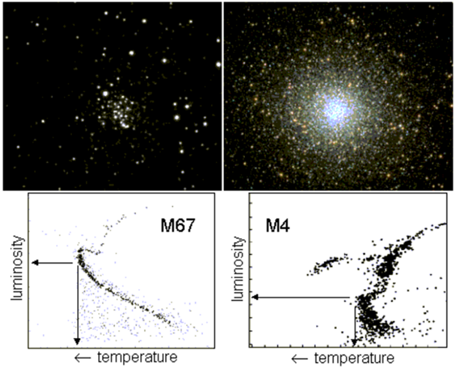

M4 CMD

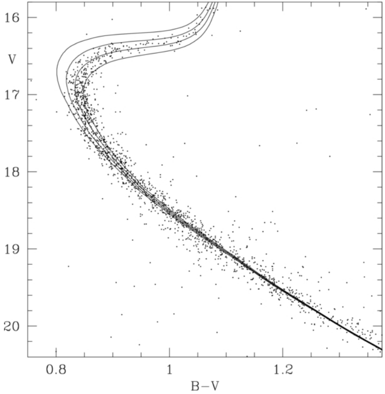

10, 11, 12 and 13 Gyr isochrones

Cluster age resolution

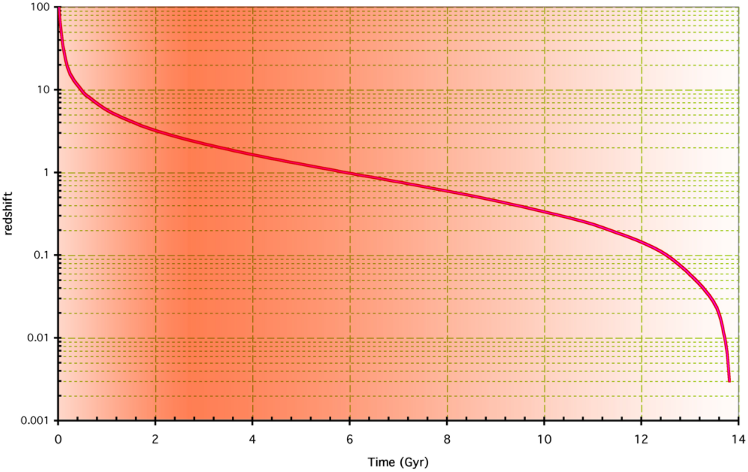

Surface brightness profile

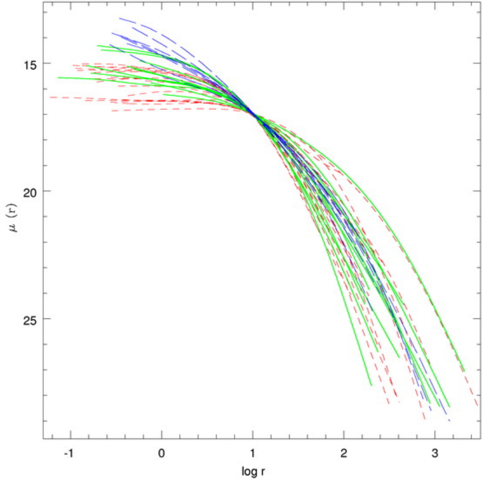

Surface brightness of 38 Galactic globular clusters imaged with the HST

Metallicity distribution

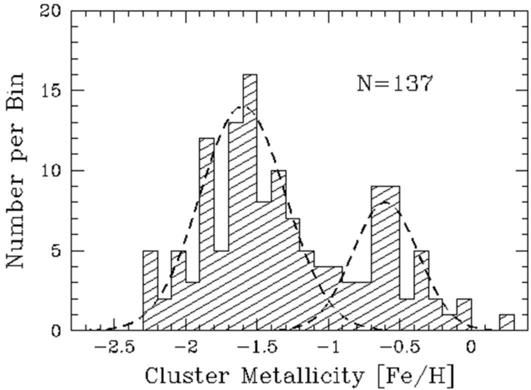

Metallicity distribution of the Galactic globular cluster system

Age-Metallicity relation

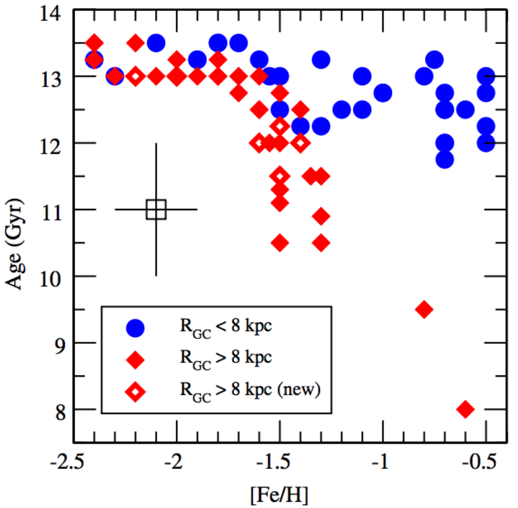

Age-Metallicity for the Galactic globular cluster from Dotter et al 2011

Star Cluster Formation

z=12

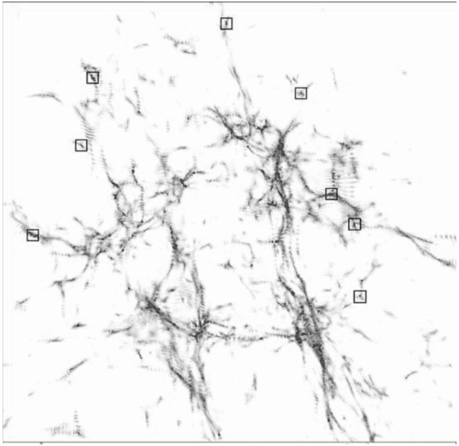

z=0

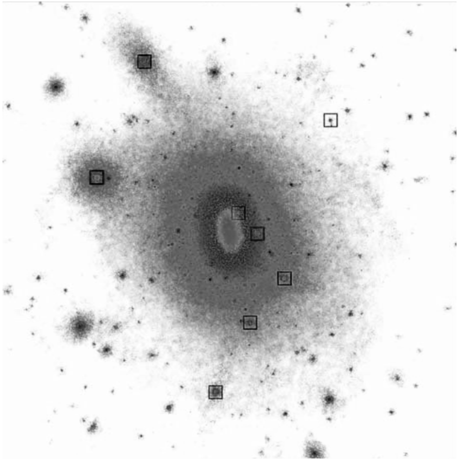

Moore et al, 2006

Star Cluster Formation

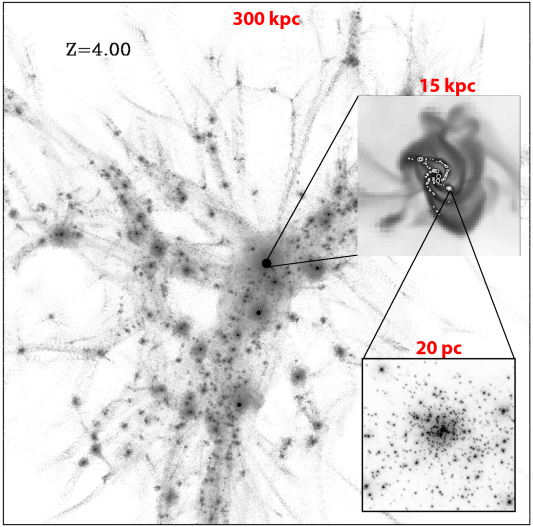

O. Gnedin, A. Kravtsov

Star Cluster disruption

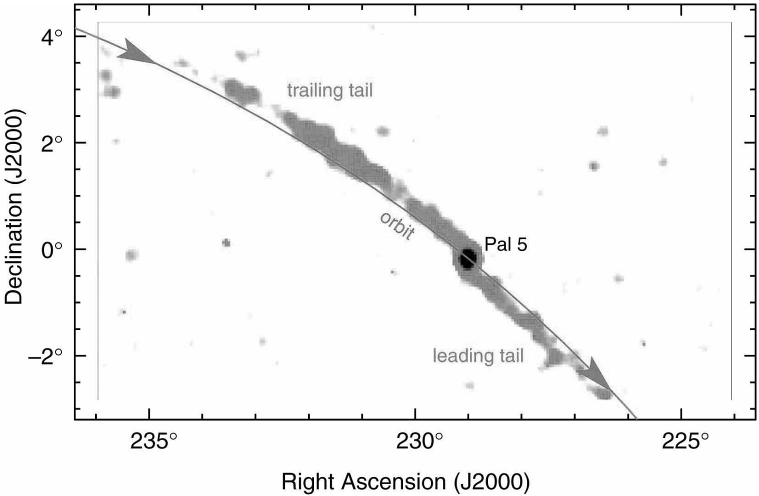

The tails of Palomar 5, (Odinkirchen et al)

King Models

Towards models of real star clusters. Lowered isothermal models

We seek models which look like an isothermal sphere at small radii (*i.e.* mostly large $\mathcal{E}$), but are less dense at large radii (smaller $\mathcal{E}$).

$$f(\mathcal{E}) = \rho_1 (2\pi\sigma^2)^{-\frac{3}{2}} e^{\mathcal{E}/\sigma^2} \quad \text{isothermal}$$

So get rid of the high v stars, since they mostly escape - and this is equivalent to choosing Φ_0 in the $\mathcal{E}$ definition to give a distribution function of the form we would like.

What we might try is to truncate the Gaussian we had before, so that

$$f(\mathcal{E}) = \begin{cases} \rho_1 (2\pi\sigma^2)^{-\frac{3}{2}} \left(e^{\mathcal{E}/\sigma^2} - 1 \right) & \mathcal{E} > 0 \\ 0 & \mathcal{E} \leq 0 \end{cases} \tag{7.1}$$

These are the **King models**.

King Models

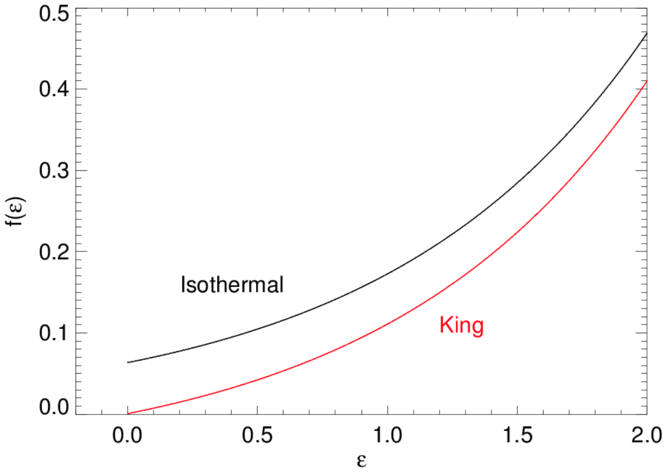

King Models

$$f(\mathcal{E}) = \rho_1 (2\pi\sigma^2)^{-\frac{3}{2}} \left(e^{\mathcal{E}/\sigma^2} - 1 \right)$$

As usual, find density at any radius by integrating over all velocities

$$\rho(\Psi) = \frac{4\pi\rho_1}{(2\pi\sigma^2)^{\frac{3}{2}}} \int_0^{\sqrt{2\Psi}} \left[\exp\left(\frac{\Psi - \frac{1}{2}v^2}{\sigma^2} \right) - 1 \right] v^2 \, dv \quad (7.2)$$

$$= \rho_1 \left[\exp\left(\frac{\Psi}{\sigma^2} \right) \mathrm{erf}\left(\frac{\sqrt{\Psi}}{\sigma} \right) - \sqrt{\frac{4\Psi}{\pi\sigma^2}} \left(1 + \frac{2\Psi}{3\sigma^2} \right) \right] \quad (7.3)$$

where

$$\mathrm{erf}(x) = \int_0^x e^{-t^2} dt.$$

Then Poisson:

$$\frac{d}{dr}\left(r^2 \frac{d\Psi}{dr} \right) = -4\pi G r^2 \rho(\Psi) \quad (7.4)$$

Solve this numerically with boundary conditions $\Psi = \Psi(0)$ and $\frac{d\Psi}{dr} = 0$ at $r = 0$.

King Models

As we integrate the ODE (7.4) outward, $\frac{d\Psi}{dr}$ decreases because initially $\frac{d\Psi}{dr} = 0$ and $\frac{d^2\Psi}{dr^2} < 0$. As Ψ decreases towards zero the range of values of v $(0, \sqrt{2\Psi})$ falls and as $\Psi \to 0$ the number of stars $\to 0$ and $\rho \to 0$ since $\rho = \int_0^{\sqrt{2\Psi}} fv^2\, dv$.

Eventually at some radius r_{t} Ψ reaches zero and the density vanishes. r_{t} is called the **tidal radius** of the cluster.

From $\rho(r) = \rho(\Psi(r))$ with the solution to (7.4) we can compute the mass inside the tidal radius $M(r_{\mathrm{t}}) = 4\pi \int_0^{r_{\mathrm{t}}} r^2 \rho_{\mathrm{K}} \mathrm{d}r$, and hence

$$\Phi(r_{\mathrm{t}}) = -\frac{GM(r_{\mathrm{t}})}{r_{\mathrm{t}}}$$

King Models

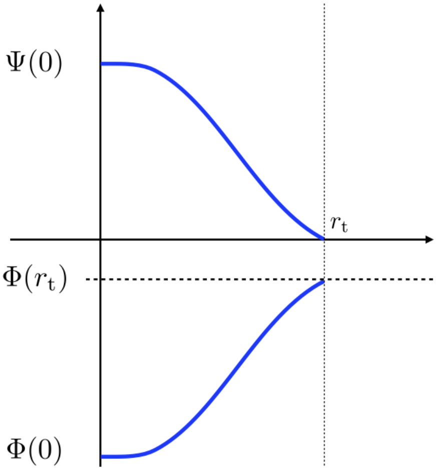

Now $\Phi(0) = \Phi(r_t) - \Psi(0)$ since we set $\Psi = 0$ at the outer edge, and $\Psi = -\Phi +$constant.

The bigger the value $\Psi(0)$ from which we start our integration, the greater will be the tidal radius, the total mass, and $|\Phi(0)|$.

King Models

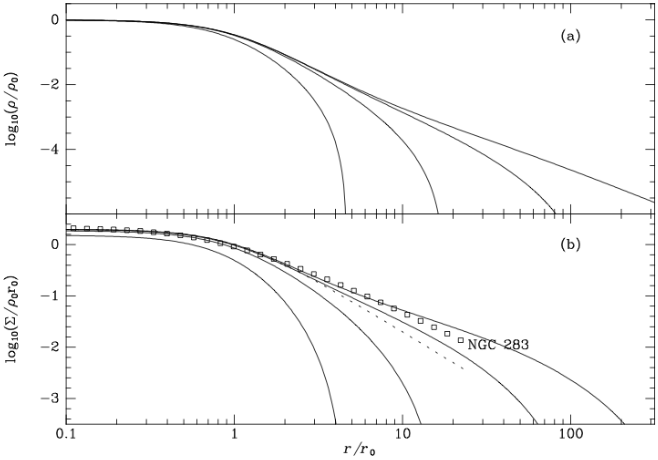

Figure 4.8 (a) Density profiles of four King models: from top to bottom the central potentials of these models satisfy $\Psi(0)/\sigma^2 = 12, 9, 6, 3$. (b) The projected mass densities of these models (full curves), and the projected modified Hubble model of equation (4.109b) (dashed curve). The squares show the surface brightness of the elliptical galaxy NGC 283 (Lauer et al. 1995).

King Models

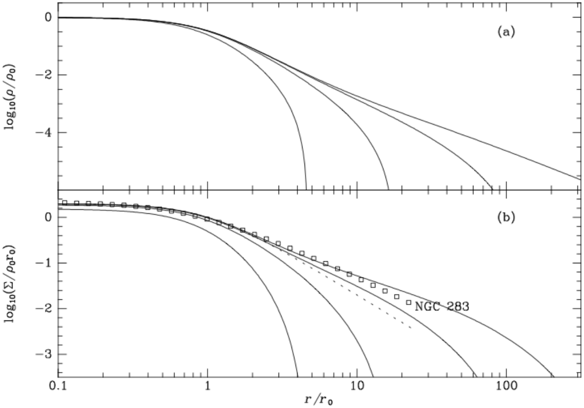

Figure 4.8 (a) Density profiles of four King models: from top to bottom the central potentials of these models satisfy $\Psi(0)/\sigma^2 = 12, 9, 6, 3$. (b) The projected mass densities of these models (full curves), and the projected modified Hubble model of equation (4.109b) (dashed curve). The squares show the surface brightness of the elliptical galaxy NGC 283 (Lauer et al. 1995).

As defined before

$$\tilde{r} = r/r_0$$

where

$$r_0 = \sqrt{\frac{9\sigma^2}{4\pi G\rho_0}}$$

i.e. r_0 s the radius at which the projected density falls to roughly half (in fact, 0.5013) of its central value. Sometimes r_0 is called the core radius in analogy with the usual observational definition.

King Models

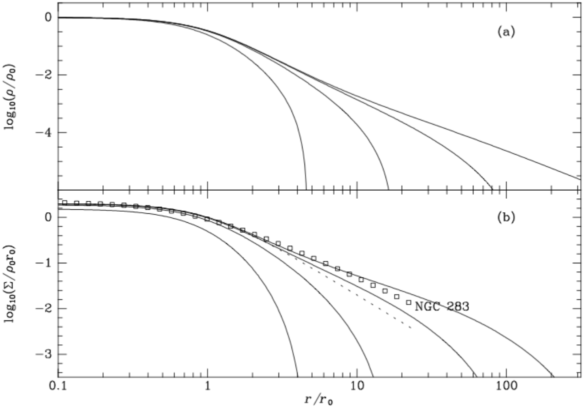

Figure 4.8 (a) Density profiles of four King models: from top to bottom the central potentials of these models satisfy $\Psi(0)/\sigma^2 = 12, 9, 6, 3$. (b) The projected mass densities of these models (full curves), and the projected modified Hubble model of equation (4.109b) (dashed curve). The squares show the surface brightness of the elliptical galaxy NGC 283 (Lauer et al. 1995).

Note also that $r_0 \neq r_c$, where r_c is the core radius which contains half the (projected) light, i.e. where $\Sigma(r_c) = \frac{1}{2}\Sigma(0)$ (see early lecture notes).

King Models

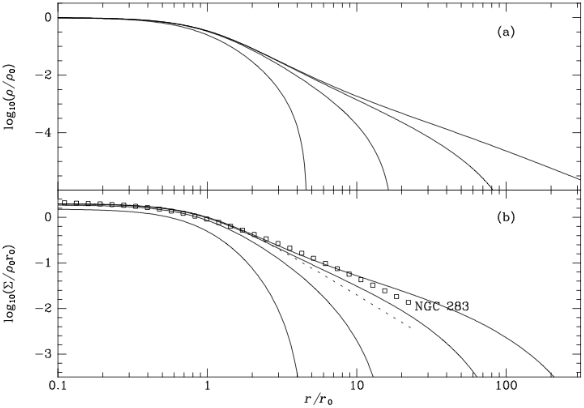

Figure 4.8 (a) Density profiles of four King models: from top to bottom the central potentials of these models satisfy $\Psi(0)/\sigma^2 = 12, 9, 6, 3$. (b) The projected mass densities of these models (full curves), and the projected modified Hubble model of equation (4.109b) (dashed curve). The squares show the surface brightness of the elliptical galaxy NGC 283 (Lauer et al. 1995).

We can define the concentration of the model

$$c = \log_{10}\left(\frac{r_t}{r_0}\right)$$

and the models are characterised by c or dimensionless $\Psi(0)/\sigma^2$.

- For globular clusters $c = 0.75$ - 1.75
- For elliptical galaxies $c \geq 2.2$

King Models

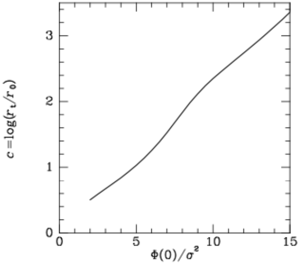

Figure 4.9 The relationship between the concentration c of a King model (eq. 4.114) and the central potential $\Psi(0)$ from which equation (4.112) is integrated.

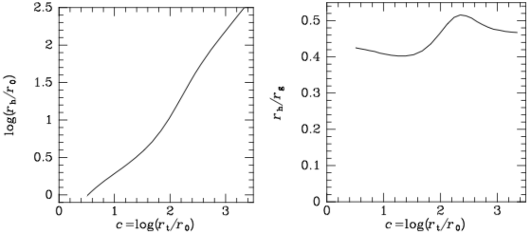

Figure 4.10 The half-mass radius r_h (left) and the ratio r_h/r_g of the half-mass radius to the gravitational radius (2.42) as a function of the concentration of a King model.

King Models

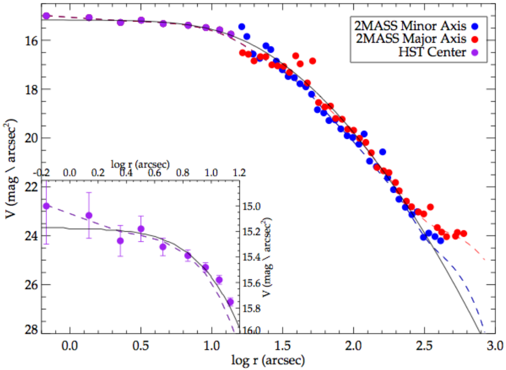

Fig. 4. The surface brightness profile of NGC 2808. The red and the blue circles mark the measurements from the 2MASS image along the major and minor axis, respectively, as well as their MGE parametrization (dashed lines). The profile obtained from the HST star catalog is shown in purple. Overplotted is the profile obtained by Trager et al. (1995) with a solid black line.

King Models

NGC 2419

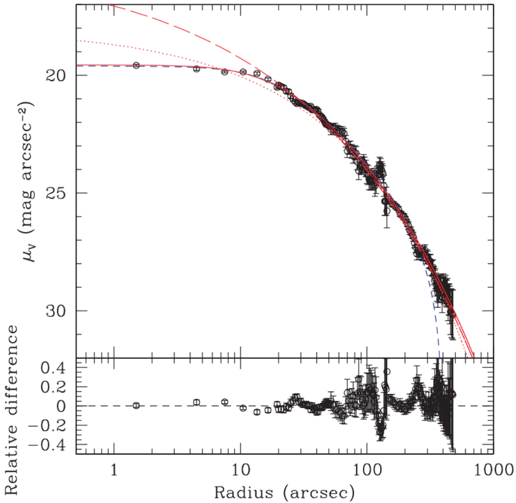

Upper panel: V-band surface brightness profile of NGC 2419 as determined by Bellazzini (2007). The blue, short-dashed curve shows the best-fitting single-mass, isotropic King model. This model cannot fit the “excess” light at large radii. The dotted and long-dashed red curves are fits of two Sérsic profiles that fit the outer parts of the cluster well but not the central region. The solid curve is a Sérsic profile with an added core of size $r_c = 14$ arcsec. It provides a good match to the density profile and is within the reported observational uncertainties at most radii (bottom panel).

King Models

NGC 2419

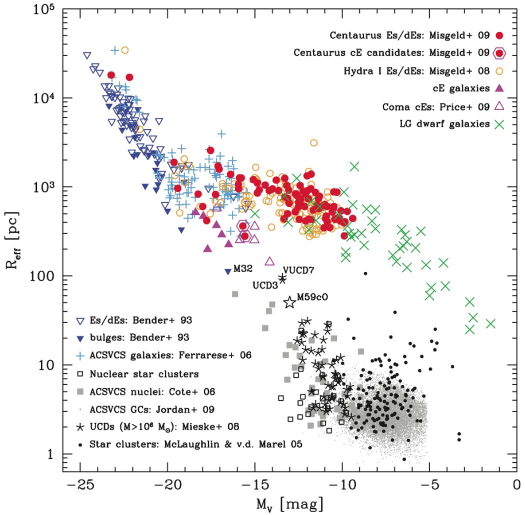

King Models

NGC 2419

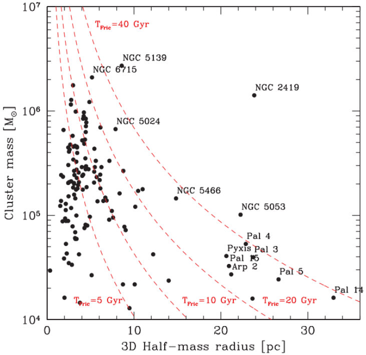

Figure 1. Dynamical friction time, $T_{\rm Fric}$, of stars against lighter DM particles for Galactic globular clusters. Most globular clusters have friction time-scales of less than a Hubble time, meaning that DM would have been depleted from their centres if they formed as a mix of DM and stars. Only a few extended clusters have friction times longer than a Hubble time and should therefore still retain DM in their centres. With the longest friction time-scale of all Galactic globular clusters, NGC 2419 is a promising target for a search for DM.

King Models

NGC 2419

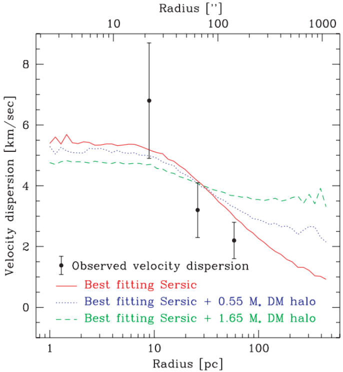

Figure 7. Observed velocity dispersion as a function of radius. The solid line shows our prediction based on the best-fitting cored Sérsic model. Dotted and dashed lines show the predicted velocity dispersion if we add NFW haloes with a scale radius of $R_S = 500$ pc and masses of $M_{DM} = 4 \times 10^6$ and $10^7\, M_\odot$ inside R_S to this model. Models with additional DM haloes significantly overpredict the velocity dispersion in the outer parts, showing that NGC 2419 does not possess a dSph-like DM halo.

King Models

The velocity dispersion in King models can also be computed by

$$\overline{v^2} = \frac{\int_0^{\sqrt{2\Psi}} \left(\exp\left[\frac{\Psi - \frac{1}{2}v^2}{\sigma^2}\right] - 1\right) v^4\, dv}{\int_0^{\sqrt{2\Psi}} \left(\exp\left[\frac{\Psi - \frac{1}{2}v^2}{\sigma^2}\right] - 1\right) v^2\, dv}$$

Note that $\overline{v^2} \to 0$ at r_t since the potential energy is already equal to the largest allowed energy there.

King Models

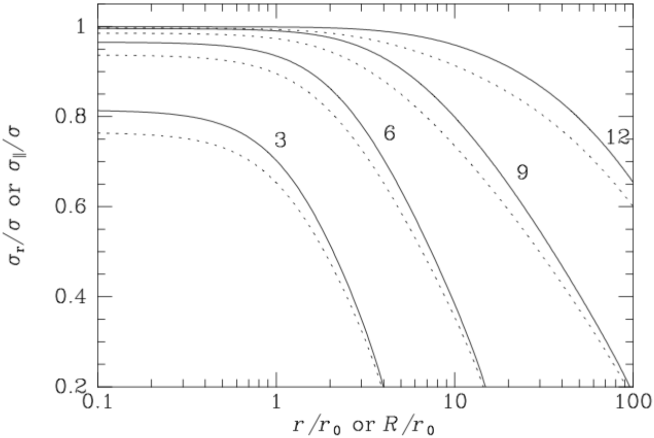

Figure 4.11 The one-dimensional velocity dispersion $\sigma_r = \sigma_\theta = \sigma_\phi$ at a given spatial radius r (full curves) and the RMS line-of-sight velocity $\sigma_{||}$ at projected radius R (dashed curves) for the King models shown in Figure 4.8. The curves are labeled by $\Psi(0)/\sigma^2$.

King Models

In this model

$$\sigma_r = \sigma_\theta = \sigma_\phi$$

Observationally, however, the velocity dispersion in the outer parts is found to be non-isotropic - there is a tendency for $\overline{v_r^2}/\overline{v_\phi^2}$ to increase with radius.

Therefore f is not just a function of $\mathcal{E}$. We'll return (briefly) to anisotropic velocity distributions later.

Jaffe Model

This is an application of Eddington formula (to show it can indeed be done).

Consider the family of double-power law models

$$\rho(r) = \frac{\rho_0}{(r/a)^{\alpha}(1 + r/a)^{\beta-\alpha}}$$

- $\beta = 4$ Dehnen (Dehnen 1993)
- $\alpha = 1, \beta = 4$ Hernquist (Hernquist 1990)
- **$\alpha = 2, \beta = 4$ Jaffe (Jaffe 1983)**
- $\alpha = 1, \beta = 3$ NFW (Navarro, Frenk & White 1993)
- $1 < \alpha < 1.5, \beta \simeq 3$ for dark haloes

So, the density is given by

$$\rho(r) = \frac{M}{4\pi r_J^3}\left(\frac{r}{r_J}\right)^{-2}\left(1 + \frac{r}{r_J}\right)^{-2} = \frac{M}{4\pi r_J^3}\frac{r_J^4}{r^2(r + r_J)^2} \tag{7.5}$$

Jaffe Model

Then we can use Poisson's equation to find $\Phi(r)$:

$$\Phi(r) = \frac{GM}{r_J} \ln\left(\frac{r}{r + r_J}\right) = -\Psi \tag{7.6}$$

Therefore

$$\frac{r}{r + r_J} = \exp\left(-\frac{\Psi r_J}{GM}\right) = e^{-\psi}$$

where $\psi = -\frac{\Psi r_J}{GM}$. Then

$$\frac{r}{r_J} = \frac{e^{-\psi}}{1 - e^{-\psi}}$$

$$1 + \frac{r}{r_J} = \frac{1}{1 - e^{-\psi}}$$

Hence

$$\rho(\psi) = \frac{M}{4\pi r_J^3} \frac{r_J^4}{r^2 (r + r_J)^2} = \frac{M}{4\pi r_J^3} \frac{\left(1 - e^{-\psi}\right)^4}{e^{-2\psi}} = \frac{M}{4\pi r_J^3} \left(e^{\frac{1}{2}\psi} - e^{-\frac{1}{2}\psi}\right)^4 \tag{7.7}$$

Jaffe Model

Let $\rho_0 = \frac{M}{4\pi r_J^3}$, and then

$$\tilde{\rho} = \frac{\rho}{\rho_0} = \left(e^{\frac{1}{2}\psi} - e^{-\frac{1}{2}\psi}\right)^4$$

Remember the Eddington's formula

$$f(\mathcal{E}) = \frac{1}{\sqrt{8}\pi^2}\left[\int_0^{\mathcal{E}} \frac{\mathrm{d}\Psi}{\sqrt{\mathcal{E}-\Psi}}\frac{\mathrm{d}^2\rho}{\mathrm{d}\Psi^2} + \frac{1}{\sqrt{\mathcal{E}}}\left(\frac{\mathrm{d}\rho}{\mathrm{d}\Psi}\right)_{\Psi=0}\right]$$

Note that $\left.\frac{d\rho}{d\psi}\right|_{\psi=0} = 0$, so we have

$$f(\mathcal{E}) = \frac{1}{\sqrt{8}\pi^2}\int_0^{\mathcal{E}} \frac{d^2\rho}{d\Psi^2}\frac{d\Psi}{\sqrt{\mathcal{E}-\Psi}} + 0$$

Jaffe Model

$$f(\mathcal{E}) = \frac{1}{\sqrt{8}\pi^2} \int_0^{\mathcal{E}} \frac{d^2\rho}{d\Psi^2} \frac{d\Psi}{\sqrt{\mathcal{E}-\Psi}} + 0$$

$$\rho(\psi) = \frac{M}{4\pi r_J^3} \left(e^{\frac{1}{2}\psi} - e^{-\frac{1}{2}\psi} \right)^4$$

$$\psi = -\frac{\Psi\, r_J}{GM}$$

Then we can use

$$\begin{aligned} \frac{d^2\tilde{\rho}}{d\psi^2} &= \frac{d^2}{d\psi^2} \left[e^{2\psi} - 4e^{\psi} + 6 - 4e^{-\psi} + e^{-2\psi} \right] \\ &= 4 \left[e^{2\psi} - e^{\psi} - e^{-\psi} + e^{-2\psi} \right] \end{aligned}$$

Jaffe Model

$$f(\mathcal{E}) = \frac{1}{\sqrt{8}\pi^2} \int_0^{\mathcal{E}} \frac{d^2\rho}{d\Psi^2} \frac{d\Psi}{\sqrt{\mathcal{E}-\Psi}} + 0$$

$$\rho(\psi) = \frac{M}{4\pi r_J^3} \left(e^{\frac{1}{2}\psi} - e^{-\frac{1}{2}\psi} \right)^4$$

$$\psi = -\frac{\Psi\, r_J}{GM}$$

With the substitution $\epsilon = \mathcal{E}/\frac{GM}{r_J}$, and $x = \sqrt{2}\sqrt{\epsilon - \psi}$ (so $dx = -\sqrt{2}\, d\psi/2\sqrt{\epsilon-\psi}$ and $\psi = \epsilon - \frac{1}{2}x^2$) we obtain

$$\begin{aligned} f(\mathcal{E}) &= \frac{4\sqrt{2}\, M}{2\sqrt{2}\pi^2 4\pi r_J^3 \left(\frac{GM}{r_J}\right)^{\frac{3}{2}}} \int_0^{\sqrt{2\epsilon}} \left[e^{2\epsilon} e^{-x^2} - e^{\epsilon} e^{-\frac{1}{2}x^2} - e^{-\epsilon} e^{\frac{1}{2}x^2} + e^{-2\epsilon} e^{x^2} \right] dx \\ &= \frac{M}{2\pi^3 (GMr_J)^{\frac{3}{2}}} \left[F_-(\sqrt{2\epsilon}) - \sqrt{2} F_-(\sqrt{\epsilon}) - \sqrt{2} F_+(\sqrt{\epsilon}) + F_+(\sqrt{2\epsilon}) \right] \end{aligned} \quad (7.8)$$

where

$$F_{\pm}(z) \equiv e^{\mp z^2} \int_0^z e^{\pm t^2}\, dt \quad \text{is Dawson's integral.}$$

$$\Rightarrow \; F_-(x) = \frac{\sqrt{\pi}}{2} e^{x^2} \mathrm{erf}(x)$$

Systems with anisotropic velocity distributions

The next most obvious constant of the motion for orbits in a system with spherical spatial symmetry is the total angular momentum **L**.

$$L^2 = L_x^2 + L_y^2 + L_z^2 = |\mathbf{r} \times \mathbf{v}|^2$$

or

$$L^2 = (rv_\theta)^2 + (rv_\phi)^2 = r^2(v_\theta^2 + v_\phi^2) = r^2 v_\perp^2$$

So consider $f \equiv f(\mathcal{E}, L^2)$, then f depends on v through $\mathcal{E} \leftrightarrow \frac{1}{2}(v_r^2 + v_\theta^2 + v_\phi^2)$ and $L^2 \leftrightarrow v_\theta^2 + v_\phi^2$. By symmetry we have $v_\theta^2 = v_\phi^2$, but $\neq v_r^2$.

Systems with anisotropic velocity distributions

For example, in isothermal models we can replace $\mathcal{E}$ with $\mathcal{E}' = \mathcal{E} - \frac{L^2}{2r_a^2}$, where r_a is some fixed radius. Then

$$
\begin{aligned}
f(\mathcal{E}, L) &= \frac{\rho_1}{(2\pi\sigma^2)^{\frac{3}{2}}} \exp\left[\frac{\mathcal{E}}{\sigma^2} - \frac{L^2}{2r_a^2\sigma^2}\right] \\
&= \frac{\rho_1 e^{\frac{\Psi}{\sigma^2}}}{(2\pi\sigma^2)^{\frac{3}{2}}} \exp\left[-\frac{v_r^2 + v_\theta^2 + v_\phi^2}{2\sigma^2} - \frac{r^2}{r_a^2}\frac{(v_\theta^2 + v_\phi^2)}{2\sigma^2}\right] \\
&= \frac{\rho_1 e^{\frac{\Psi}{\sigma^2}}}{(2\pi\sigma^2)^{\frac{3}{2}}} \exp\left(-\frac{v_r^2}{2\sigma^2}\right) \exp\left[-\left(1 + \frac{r^2}{r_a^2}\right)\frac{(v_\theta^2 + v_\phi^2)}{2\sigma^2}\right]
\end{aligned}
$$

Using this, we can look at the transverse *vs* radial velocity dispersions

$$
\overline{v_\theta^2} = \frac{\iiint_{-\infty}^{\infty} v_\theta^2 f(\mathcal{E}, L)\, dv_r\, dv_\theta\, dv_\phi}{\iiint_{-\infty}^{\infty} f(\mathcal{E}, L)\, dv_r\, dv_\theta\, dv_\phi}
$$

Systems with anisotropic velocity distributions

Then

$$\frac{\overline{v_\theta^2}}{\overline{v_r^2}} = \frac{\int_{-\infty}^{\infty} v_\theta^2 \exp\left[-\left(1+\frac{r^2}{r_a^2}\right)\frac{v_\theta^2}{2\sigma^2}\right]\,dv_\theta \Big/ \int_{-\infty}^{\infty} \exp\left[-\left(1+\frac{r^2}{r_a^2}\right)\frac{v_\theta^2}{2\sigma^2}\right]\,dv_\theta}{\int_{-\infty}^{\infty} v_r^2 \exp\left[-\frac{v_r^2}{2\sigma^2}\right]\,dv_r \Big/ \int_{-\infty}^{\infty} \exp\left[-\frac{v_r^2}{2\sigma^2}\right]\,dv_r}$$

where the velocity integrals extend to infinity for the isothermal model since the mass is infinite.

$$\frac{\overline{v_\theta^2}}{\overline{v_r^2}} = \left[\frac{1}{2\left(1+\frac{r^2}{r_a^2}\right)/2\sigma^2}\right] \Big/ \frac{1}{2(1/2\sigma^2)} = \frac{1}{1+\frac{r^2}{r_a^2}} \qquad (7.9)$$

So as

$$r \to 0 \quad \frac{\overline{v_\theta^2}}{\overline{v_r^2}} \to 1$$

i.e. at small radii it is **isotropic**, but as $\frac{r}{r_a}$ increases $\frac{\overline{v_\theta^2}}{\overline{v_r^2}}$ decreases, so becomes **anisotropic** in the sense that the orbits become more radial.

Systems with anisotropic velocity distributions

Then

$$\frac{\overline{v_\theta^2}}{\overline{v_r^2}} = \frac{\int_{-\infty}^{\infty} v_\theta^2 \exp\left[-\left(1+\frac{r^2}{r_a^2}\right)\frac{v_\theta^2}{2\sigma^2}\right] dv_\theta / \int_{-\infty}^{\infty} \exp\left[-\left(1+\frac{r^2}{r_a^2}\right)\frac{v_\theta^2}{2\sigma^2}\right] dv_\theta}{\int_{-\infty}^{\infty} v_r^2 \exp\left[-\frac{v_r^2}{2\sigma^2}\right] dv_r / \int_{-\infty}^{\infty} \exp\left[-\frac{v_r^2}{2\sigma^2}\right] dv_r}$$

where the velocity integrals extend to infinity for the isothermal model since the mass is infinite.

$$\frac{\overline{v_\theta^2}}{\overline{v_r^2}} = \left[\frac{1}{2\left(1+\frac{r^2}{r_a^2}\right)/2\sigma^2}\right] \Big/ \frac{1}{2(1/2\sigma^2)} = \frac{1}{1+\frac{r^2}{r_a^2}} \qquad (7.9)$$

So as

$$r \to 0 \quad \frac{\overline{v_\theta^2}}{\overline{v_r^2}} \to 1$$

i.e. at small radii it is **isotropic**, but as $\frac{r}{r_a}$ increases $\frac{\overline{v_\theta^2}}{\overline{v_r^2}}$ decreases, so becomes **anisotropic** in the sense that the orbits become more radial.

Michie Models

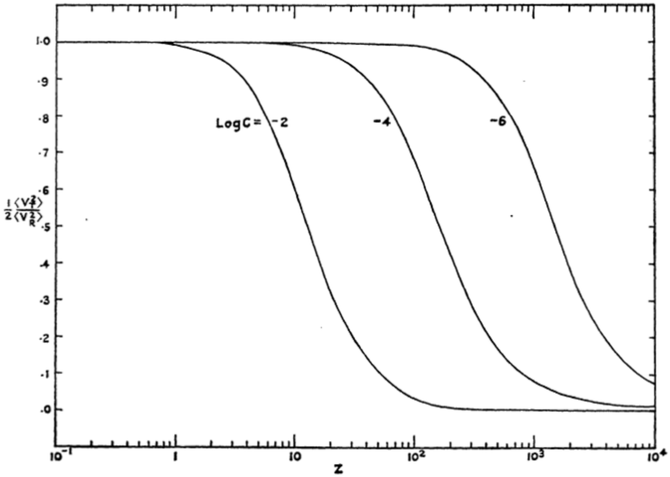

FIG. 4.—*Here is plotted the ratio of the tangential to the radial average energy, versus z. This is an index of the degree of orbital eccentricity at different distances from the centre.*

Systems with anisotropic velocity distributions

These give rise to a generalisation of the King model called Michie models, where

$$f_{\mathrm{M}}(\mathcal{E}, L) = \begin{cases} \rho_1 (2\pi\sigma^2)^{-\frac{3}{2}} \exp\left(-\frac{L^2}{2r_a^2\sigma^2}\right)\left[e^{\frac{\mathcal{E}}{\sigma^2}} - 1\right] & \mathcal{E} > 0 \\ 0 & \mathcal{E} \leq 0 \end{cases}$$

As $r_a \to \infty$ this model becomes the King model, as you would expect.

In the Michie model, the velocity distribution is isotropic at the centre, but nearly radial in the outer parts, with a transition region near the anisotropy radius $r = r_a$.

Is this expected? Cluster evolution - encounters tend to fling stars out, so will have radial orbits at the outside. However "encounters" mean it is not "collisionless".
... so we do need to consider evolution of clusters in time.

Systems with anisotropic velocity distributions

These give rise to a generalisation of the King model called Michie models, where

$$f_{\mathrm{M}}(\mathcal{E}, L) = \begin{cases} \rho_1 (2\pi\sigma^2)^{-\frac{3}{2}} \exp\left(-\frac{L^2}{2r_a^2\sigma^2}\right)\left[e^{\frac{\mathcal{E}}{\sigma^2}} - 1\right] & \mathcal{E} > 0 \\ 0 & \mathcal{E} \leq 0 \end{cases}$$

As $r_a \to \infty$ this model becomes the King model, as you would expect.

In the Michie model, the velocity distribution is isotropic at the centre, but nearly radial in the outer parts, with a transition region near the anisotropy radius $r = r_a$.

Is this expected? Cluster evolution - encounters tend to fling stars out, so will have radial orbits at the outside. However “encounters” mean it is not “collisionless”.
… so we do need to consider evolution of clusters in time.

Modelling Cluster Evolution

Two main approaches: Fokker-Planck equation and Direct N-body

1 Fokker-Planck equation: start from collisionless Boltzmann equation $\frac{df}{dt} = 0$,

$$\frac{\partial f}{\partial t} + \mathbf{v} \cdot \nabla f - \nabla \Phi \cdot \frac{\partial f}{\partial \mathbf{v}} = 0$$

but relax assumption $\ddot{\mathbf{r}} = -\nabla \Phi$ to allow for the fact that phase space density near a star can be changed due to encounters. Find that

$$\frac{df}{dt} = \Gamma(f) \neq 0$$

where Γ is obtained from the probability of particles being scattered out of and in to the phase space neighbourhood of a given particle. This requires knowledge of cross-sections for all types of stellar encounter.

Modelling Cluster Evolution

2 Direct N-body methods (Aarseth 1963++++) where sum up forces on each star to calculate acceleration and orbit.

Models now include stellar evolution (Tout), stellar mass loss, tidal dissipation and capture, collisions, binary evolution, mass transfer, gravitational radiation, disruption of binaries, tidal stripping by an external potential. To integrate orbits of stars from hard binaries to halo escapes requires very accurate N-body code. Can study small globulars correctly, and improving all the time.

N-body vital to

- calibrate Fokker-Planck methods.
- discover any new effects (since only minimal assumptions are made in advance i.e. Newtonian gravity).

Modelling Cluster Evolution

Although N-body simulations are simple in principle, many sophisticated techniques are needed to make them efficient enough to be useful.

1. The central core of the cluster is much denser than its outer parts, so the timestep required for stars in the core must be much shorter than the timestep for most other stars. This problem is solved by assigning each star its own time-step.
2. Binary and triple stars can be formed with orbital periods far shorter than the crossing time. These require special treatment, by a combination of analytical solutions of the Kepler problem and other techniques.
3. The computation of the force by direct summation requires of order N^2 operations, while advancing the orbits requires only of order N operations. Thus the force computation takes far more time than the orbit calculation. This problem can be addressed in either hardware or software.

Modelling Cluster Evolution

- The hardware solution is to develop **special-purpose computers** that parallelize and pipeline the force calculation, leaving the much easier task of advancing the orbits to a general-purpose host computer.
- The software solution is to separate the rapidly varying forces from the small number of nearby particles and the slowly varying forces from the large number of distant ones, using a neighbor scheme.

Modelling Cluster Evolution

A super computer with thousands of cores

Globular cluster evolution

Relaxation times

So far we have used the collisionless Boltzmann equation, where the assumption is that stars give rise to a smooth gravitational potential profile. This is invalidated by stellar encounters on timescales $t_{\rm relax}$.

We found

$$t_{\rm relax} \simeq \frac{0.1N}{\ln N} t_{\rm cross}$$

where

$$t_{\rm cross} \simeq \sqrt{\frac{R^3}{GM}}$$

For a globular cluster we might take $r_t \sim 50\,\text{pc}$, $M \sim 6 \times 10^5\,\text{M}_\odot$, $N \sim 10^6$ stars, and so $t_{\rm cross} \sim 7 \times 10^6\,\text{yr}$ and $t_{\rm relax} \sim 5 \times 10^{10}\,\text{yr}$, which is somewhat greater than the age ($\sim 10^{10}\,\text{yr}$).

Those with long memories will note that this timescale is a factor of 10 or so longer than the estimate we obtained earlier - there we used r_t which was $5\times$ smaller, and used an observed velocity! So globular clusters as a whole may be nearly relaxed - with $t_{\rm relax} \sim$ their age.

Globular cluster evolution

Relaxation times

In the core it is less marginal. $r_c \simeq 1.5\,\text{pc}$, $N_c \simeq 10^4$, $M_c \simeq 8 \times 10^3\,\mathrm{M}_\odot$, and so $t_{\text{relax}} \sim 3 \times 10^7\,\text{yr}$, which is much less than the age.

For open clusters, $N \simeq 100$, $t_{\text{cross}} \simeq 10^6\,\text{yr}$, age$\simeq 10^8\,\text{yr}$, which $\Rightarrow t_{\text{relax}} \simeq 2 \times 10^6\,\text{yr}$, which is considerably less than the age estimate.

So for open clusters, and at least the inner parts of globular clusters, we must take account of stellar encounters.

Globular cluster evolution

Relaxation

What are the effects of encounters on a star cluster?

1. Relaxation As in a gas, we expect evolution towards a state of higher entropy. Expect energy to be passed from "hotter" to "colder" parts of the cluster, where "hotter" $\leftrightarrow$ higher velocity dispersion σ. A cluster can be thought of as core (with high $\overline{v^2}$) and halo (with low $\overline{v^2}$), so core loses energy to the halo.

But from the virial theorem we know that the kinetic energy $\simeq$ |potential energy|, so $\frac{1}{2}M\overline{v^2} \simeq \frac{GM^2}{R}$. If we remove energy from the core it must contract, so $R\downarrow$, and in so doing $\overline{v^2}\uparrow$ - i.e. a self-gravitating system has negative heat capacity. There is no equilibrium configuration, and instead there is continual transfer of energy from an ever hotter, denser core to the halo (core collapse, see later).

Globular cluster evolution

Escape of stars

2. Escape of Stars Since a globular cluster has finite mass, it has a finite escape velocity.

- From time to time, encounters give a star enough energy that it can escape, so have a steady evaporation of stars.

  At position $\mathbf{r}$, the escape speed $v_e^2(\mathbf{r}) = -2\Phi(\mathbf{r})$.
  The mean square escape speed is

$$< v_e^2 > = \frac{\int \rho(\mathbf{r}) v_e^2(\mathbf{r}) d^3\mathbf{r}}{\int \rho(\mathbf{r}) d^3\mathbf{r}} = -\frac{2\int \rho(\mathbf{r})\Phi(\mathbf{r}) d^3\mathbf{r}}{M} = -4\frac{\Omega}{M}$$

  where Ω is the potential self-energy.

Globular cluster evolution

Escape of stars

The virial theorem: $-\Omega = 2T$ where $T = \frac{1}{2}M < v^2 >$ is the kinetic energy, and hence

$$< v_{\rm e}^2 >= 4 < v^2 >$$

For a Maxwellian distribution in velocity the fraction of particles with speeds exceeding twice the RMS speed is $\epsilon = 7.4 \times 10^{-3}$ (Problem set 3).

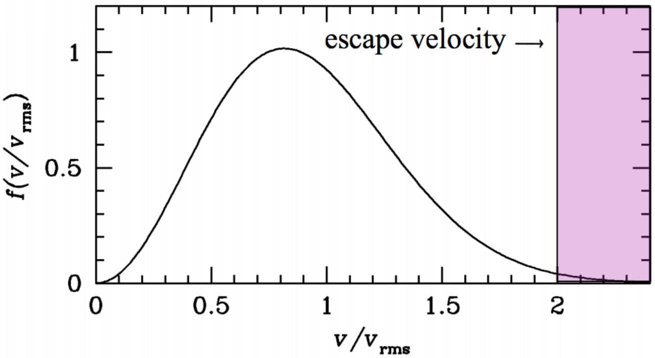

Globular cluster evolution

Escape of stars

Roughly, evaporation removes ϵN stars on a timescale $t_{\rm relax}$, so

$$\frac{dN}{dt} = -\frac{\epsilon N}{t_{\rm relax}} = -\frac{N}{t_{\rm evap}}$$

$$\rightarrow t_{\rm evap} = \epsilon^{-1} t_{\rm relax} \simeq 136\, t_{\rm relax}$$

Evaporation will set upper limit to the lifetime of a bound stellar system of $\sim 10^2 t_{\rm relax}$.

- Another mechanism for stars to escape is via close encounters. Rare, but can lead to stars escaping with $v >> v_{\rm e}$ rather than trickling out with $E \simeq 0$ by evaporation.
- Also supernovae result in neutron stars which can have high velocities, and so these too escape with high velocities.

Globular cluster evolution

Escape of stars

Roughly, evaporation removes ϵN stars on a timescale $t_{\rm relax}$, so

$$\frac{dN}{dt} = -\frac{\epsilon N}{t_{\rm relax}} = -\frac{N}{t_{\rm evap}}$$

$$\rightarrow t_{\rm evap} = \epsilon^{-1} t_{\rm relax} \simeq 136\, t_{\rm relax}$$

Evaporation will set upper limit to the lifetime of a bound stellar system of $\sim 10^2 t_{\rm relax}$.

- Another mechanism for stars to escape is via close encounters. Rare, but can lead to stars escaping with $v >> v_{\rm e}$ rather than trickling out with $E \simeq 0$ by evaporation.
- Also supernovae result in neutron stars which can have high velocities, and so these too escape with high velocities.

Globular cluster evolution

Core collapse

3. Core Collapse [see Binney & Tremaine]
A cluster evaporates on a timescale $\sim 100t_{\rm relax}$ in the absence of an external tidal field.

Total energy of cluster $E = -kGM^2/R$, where k is a constant.

Most stars which evaporate have energy $E \simeq 0$ (i.e. they just manage to escape), so the cluster evolves at constant energy. Thus

$$R \propto M^2$$

and

$$\rho \propto \frac{M}{R^3} \propto M^{-5}$$

So as $M \to 0$, $R \to 0$ and $\rho \to \infty$!

Modelling Cluster Evolution

Core collapse

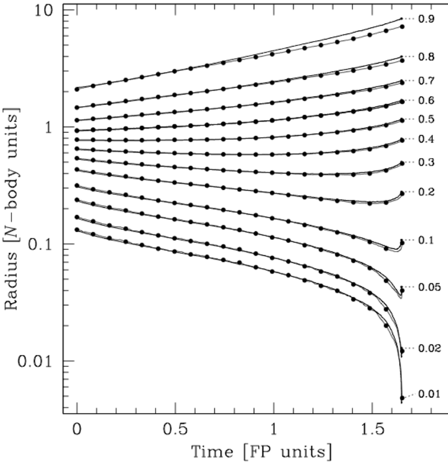

B&T Figure 7.4

The evolution of the mass distribution in an isolated cluster that began as a Plummer model. The outer half of the cluster expands, due to the gradual growth of the halo as core stars diffuse towards the escape energy. At the same time, the center contracts; the central 1% of the mass contracts by a factor $k > 30$, corresponding to an increase in the central density by a factor $k^3 > 3 \times 10^4$!

Globular cluster evolution

Core collapse

In fact what happens is not that the whole cluster collapses, but only the core does.

- Get core-halo structure from evaporation of stars from the core into the halo, and the stars ejected from the core share energy with halo stars.
- Distribution of stars (even in the halo) at late times is governed by core interactions.
- Some core stars escape altogether but still do in $|\Phi|$ work on remaining stars as they leave.

Transfer of heat leads to **gravothermal catastrophe** (negative heat capacity of the core), and core collapse follows after 10 - 20 $t_{\rm relax}$.

Globular cluster evolution

Core collapse

What halts core collapse? As the density increases, interactions become more important. Primordial hard binaries (if present) can prevent/delay core collapse by providing energy input. 3-body (rare) and (more frequent) tidal capture binaries form and halt core collapse, and also drive subsequent core expansion.

Consider 3 stars with kinetic energies K_1, K_2 and K_3, two stars form a binary with energy $E_b < 0$ and the kinetic energy of the center of mass K_b, while the third star now has K_3'
Conservation of energy requires:

$$K_1 + K_2 + K_3 = K_b + E_b + K_3'$$

Hence

$$K_b + K_3' > K_1 + K_2 + K_3$$

Therefore creation of binaries is a **heat source**.

Globular cluster evolution

Core collapse

And so is interaction with binaries!

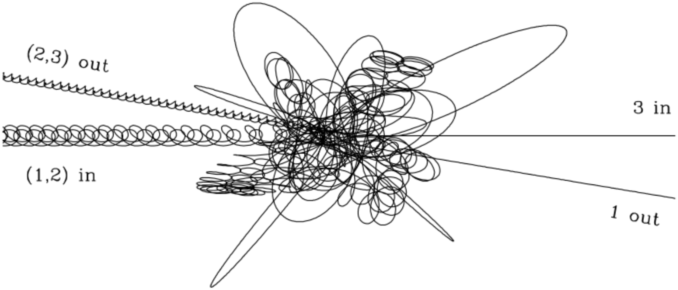

Figure 7.8 An interaction between a hard binary and a field star. All three stars have equal mass and the orbits are plotted in the center-of-mass frame. The binary, containing stars 1 and 2, enters from the left; the single star (labeled 3) enters from the right. After a complicated interaction, star 1 escapes, leaving 2 and 3 behind as a newly formed binary. After Hut & Bahcall (1983).

Exchange. Ejected star has speed of order of orbital velocity.

Globular cluster evolution

Core collapse

What happens after the collapse?

Binaries in the core pump kinetic energy into the cluster. The cluster expands.

Globular cluster evolution

Core collapse

Gravothermal oscillations

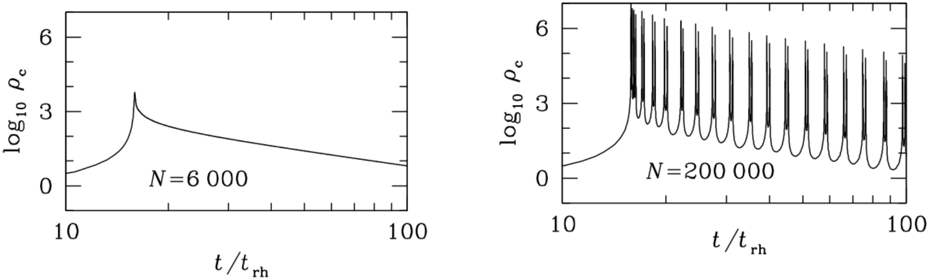

B&T, Figure 7.6s

Globular cluster evolution

Mass segregation

4. Mass Segregation Stars in clusters do not all have the same mass - in a globular cluster they range from $\sim 0.2\,M_\odot$ to $0.8\,M_\odot$. Encounters lead to equipartition of kinetic energy, so $\overline{v^2} \propto m^{-1}$, and consequently massive stars (or binaries) acquire lower velocities and sink towards the centre, so have mass segregation.
Theorem: stars in cluster will end up having same average kinetic energy.

Likewise low mass stars are preferentially sent towards the halo and eventually evaporate. Since low-mass stars have high M/L, this effect lowers the overall M/L of globular clusters.

[In globular clusters, most stars have masses in the range 0.2 - $0.8\,M_\odot$ - thos with masses $> 0.8\,M_\odot$ have already evolved, and those with masses $< 0.2\,M_\odot$ are likely to have evaporated.]

Globular cluster evolution

Mass segregation in M 10

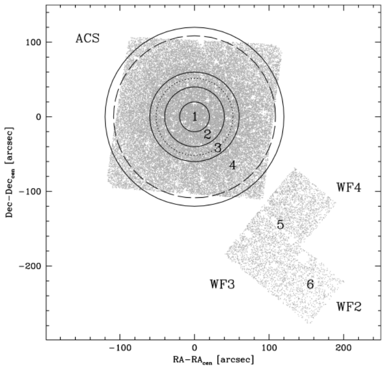

Figure 1. Map of the entire *HST* data set used in this work. The position of each camera is labeled. The nominal core radius ($r_c = 0\rlap{.}'86$) and half mass radius ($r_h = 1\rlap{.}'81$) taken from Harris (1996) are showed with dotted and dashed circles, respectively. The full circles define the four annuli in which we divided the ACS photometry. For details on the radial division criteria of ACS and WFPC2 see Section 2.3.

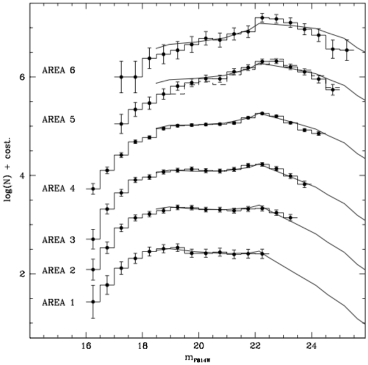

Figure 5. m_{F814W} OLFs of M10, divided in different areas (see Section 3). The measurements as reported in Table 2 (full circles in the plot) are shifted by an arbitrary amount to make the plot more readable. The TLFs that best fit the data are shown as solid lines. The index of their corresponding power-law MF is, from bottom to top, $\alpha = 0.7, 0.4, 0.1, -0.3, -0.6, -0.9$. A positive index means that the number of stars decreases with mass. All but the innermost LF reach a mass of 0.2 $M_\odot$.

Beccari et al, 2010

Globular cluster evolution

Mass segregation in M 10

No primordial binaries

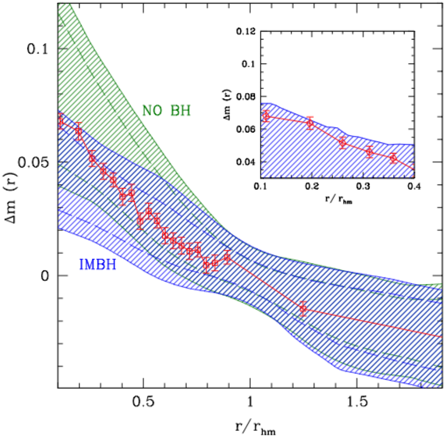

With primordial binaries

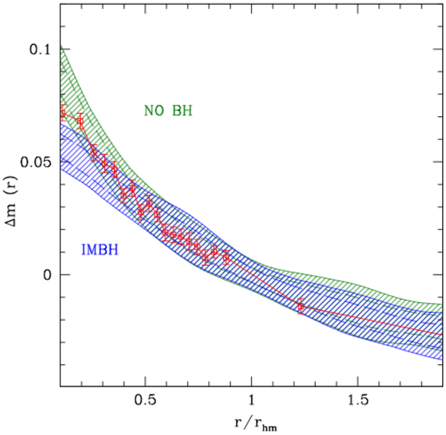

Beccari et al, 2010

Globular cluster evolution

Tidal stripping

5. Tidal Stripping

As a cluster orbits a galaxy (e.g. a globular cluster around the Milky Way) some loosely bound stars may be captured by the galaxy and removed from the star cluster. The radius at which this occurs is the tidal radius.

Consider a point mass galaxy, mass M_{G} at a distance R_{G} from the centre of a globular cluster. For a star lying along the line of centres the tidal force is

$$\begin{aligned} F_{\mathrm{t}} &= \frac{GM_{\mathrm{G}}}{R_{\mathrm{G}}^2} - \frac{GM_{\mathrm{G}}}{(R_{\mathrm{G}}+r)^2} \\ &\simeq \frac{GM_{\mathrm{G}}}{R_{\mathrm{G}}^2} - \frac{GM_{\mathrm{G}}}{R_{\mathrm{G}}^2}\left(1 - 2\frac{r}{R_{\mathrm{G}}}\right) \\ &= \frac{2rGM_{\mathrm{G}}}{R_{\mathrm{G}}^3} \end{aligned}$$

Globular cluster evolution

Tidal stripping

At some radius r_{t} this force balances the attraction due to the cluster i.e.

$$\frac{2rGM_{\mathrm{G}}}{R_{\mathrm{G}}^3} = \frac{GM_{\mathrm{C}}}{R_{\mathrm{t}}^2}$$

$\Rightarrow$

$$r_{\mathrm{t}} = \left(\frac{M_{\mathrm{C}}}{2M_{\mathrm{G}}}\right)^{\frac{1}{3}} R_{\mathrm{G}}$$

More generally, tidal stripping occurs outside a radius R_{t} within which the cluster density $\approx$ the mean density of the galaxy within the cluster orbit.
Evidence:

- tidal truncation (e.g King models fit old clusters better)
- tidal tails around Pal 5

Globular cluster evolution

Encounters with Binary Stars

6. Encounters with Binary Stars

General encounters between single stars and binaries are difficult to treat.

There are two broad categories:

1. Soft binaries (wide)
2. Hard binaries (close)

Globular cluster evolution

Encounters with Binary Stars

- Soft binaries (wide)
  $\frac{GM}{a} << \ < v^2 >$, so star #3 is not strongly gravitationally focussed.

  Since star #3 travels faster than the orbital motion of #1 and #2, the encounter tends to transfer energy into orbital motion of the binary (equipartition with reduced particle). Hence *soft binaries become softer* and will ulimately dissolve whem $E_{\mathrm{binary}} > 0$ (in centre of mass frame).

Globular cluster evolution

Encounters with Binary Stars

- Hard binaries (close)
  $\frac{GM}{a} >> \ < v^2 >$, so there is strong focussing of star #3's orbit, and it ends up in the vicinity of #1 and #2 with velocity $\simeq$ their orbital velocity. The three then form an unstable triple system until one star acquires enough energy to escape. Since the kinetic energy of the ejected star is generally greater than that of the incoming star, the energy E of the binary decreases, i.e. $|E|$ increases so it becomes more tightly bound. So *hard binaries get harder*. Note that the remaining binary can be any pairing from the three stars, not necessarily the original pair.

Globular cluster evolution

Encounters with Binary Stars

Soft binaries becoming softer, and hard binaries harder, together are sometimes referred to as **Heggie's law**.
In globular clusters the hard/soft transition occurs at separations of about 10 au.
Hard binaries act as energy sources, and thus can end core collapse. Encounters with single stars give kinetic energy to the single star which emerges as the binary orbital speed increases - also binaries are more massive and tend to sink to the core.
Cluster K.E.$\sim \frac{1}{2} M v^2 \sim \frac{1}{2} 10^5\,\mathrm{M}_\odot \times (10\,\mathrm{km\,s^{-1}})^2 = T$
Binding energy $\sim -T \simeq 10^{43}$ J.
The maximum energy which can be extracted from a hard binary is $\sim \frac{GM^2}{2R}$ where M is the mass of each star and R the radius for each. Putting in solar values gives us $E \sim 10^{41}$ J.
So ~ 100 binaries contain enough binding energy to disrupt a cluster!
So the presence of binaries strongly affects cluster evolution (but note that as the binary shrinks the effective cross-section goes down).

Globular cluster evolution

7. Binary Formation through inelastic encounters

Not all binaries were formed at the the birth of the cluster.

- Dynamical capture. Requires three independent stars in a gravitationally focussed interaction, so three stars in a region of size $\sim \frac{Gm}{<v^2>} \sim 10\,\mathrm{au}$, so this is rare. Result is a temporary triple followed by breakup into binary plus ejected single star.
- Tidal capture - inelastic encounters. If two stars pass close to each other they raise tides in each other's envelopes. Dissipation of energy in the envelope results in irreversible transfer of orbital energy of the two-body system into heat. Note that for this to occur at all the stars have to pass within a few stellar radii of each other. Since
$$\frac{gM_*}{R_*} \simeq 600\,\mathrm{km\,s^{-1}} >> \; < v^2 > \simeq 10\,\mathrm{km\,s^{-1}}$$
these are highly gravitationally focussed, and only a small fraction of the pericentre kinetic energy needs to be dissipated in order for the resulting orbit to have $E < 0$. Then an unbound orbit $\rightarrow$ bound orbit i.e. capture.

This mechanism is much more important for binary formation than dynamical capture. Estimate of rate (problem set 3).

Globular cluster evolution

Binary Formation through inelastic encounters

Right at the beginning of the course we saw that without gravitational focussing the probability of a collision was about 1 per 10^6 stars in a cluster lifetime (this assuming a cross-section of $\pi(2R_*)^2$).
If we include focussing, then conservation of angular momentum $\Rightarrow bv = 2R_* v_*$, where $v_*^2 = \frac{2Gm_*}{R_*}$ and v is the relative velocity when the two stars are far apart.
$\Rightarrow \frac{b}{2R_*} = \frac{v_*}{v}$ i.e. the cross-section is increased by a factor

$$\left(\frac{v_*}{v}\right)^2 \simeq \left(\frac{600}{15}\right)^2 = 1600$$

To form binaries by tides need $R_{\rm min} \simeq \text{few} \times R_*$, so more frequent.
Binary formation manifested in low-mass X-ray binaries in globular clusters (Fabian, Pringle & Rees, 1975) - close binaries involving neutron star and low-mass stellar companion.
Another product of inelastic encounters are physical collisions - rarer than tidal capture. This may explain Blue Stragglers in clusters - anomalously blue stars given the turn-off age of the cluster. Should have evolved long ago if formed 10Gyr ago, so could have formed more recently via main sequence star collisions.

Globular cluster evolution

8. Other Processes

Stellar Evolution: Stars lose mass via stellar winds, and if the become supernovae. Ejecta travels at a few$\times 10\,\mathrm{km\,s^{-1}}$, and so will escape the cluster, thus reducing the gravitational mass remaining in the cluster. Consequently the cluster expands in response to this mass loss.

Globular cluster evolution

- Evaporation
- Gravo-thermal instability
- Equipartition

Globular cluster evolution